Molecular Dynamics Simulations of Water at NaCl(001) and NaCl(011) Surfaces

Hiroyuki Shinto, Takashi Sakakibara, and Ko Higashitani*

Division of Chemical Engineering, Graduate School of Engineering, Kyoto University, Yoshida, Sakyo-ku, Kyoto, 606-8501 Japan

Received: August 27, 1997; In Final Form: January 5, 1998

The characteristics of water molecules near the (001) and (011) faces of NaCl crystals at 298 K were investigated, using classical molecular dynamics simulation. It was found that no ion is dissolved from the crystals into water during 10 ps and so the NaCl(001) and NaCl(011) surfaces without any lattice defect are stable in water, at least within the period of our computer experiments. The successive simulation exhibited that (1) water molecules in the first two layers near the crystal surfaces reduce their diffusivity and are regarded as "solidlike", but a slight difference in the features between NaCl(001) and NaCl(011) surfaces causes the significant difference in the interactions between a water molecule and the surfaces, the number of adsorbed layers of water, the positions of water molecules, the perturbation of the hydrogen-bonding network, and the detailed diffusional motion near the surface, and (2) water molecules in the central region of the water lamina confined between the two surfaces can be regarded as bulk with respect to the static property, but their dynamical properties are still influenced by the existence of the crystal surfaces.

1. Introduction

To understand the structure and dynamics of water adjacent to a surface is of fundamental importance in wide regions of science and engineering, such as electrochemistry, geochemistry, colloid science, and crystallography. Molecular dynamics (MD) simulation is a good tool to study the liquid/vapor,[1,2] liquid/liquid,[3−5] and liquid/solid[6−17] interfaces and lipid bilayer[18−20] at a molecular level. As far as liquid/solid interfaces are concerned, several MD simulations have been performed to elucidate the features of water mainly near the hydrophobic surfaces[6,7] and various electrodes of Pt, Ag, Cu, and Ni.[8−12] However, very few studies on the polar or hydrophilic surfaces have been reported except the studies on the surfaces of NaCl,[13] MgO,[14] SiO_2,[15,16] lecithin,[15,16] urea,[17] and fully hydroxylated silica.[7] It was found that the density profile in the three layers of water molecules next to the surface oscillates, accompanying significant structural change, and that the diffusional motion of water near the surface is very sensitive to the nature of the surface. The density oscillation was confirmed experimentally by X-ray scattering measurements of water at charged Ag(111) surfaces.[21] These results indicate that the structural and dynamical properties of water at interfaces are determined by water−water and water−surface interactions and the detailed structure of the surface.

We are interested, especially, in water/NaCl interfaces from a crystallographical point of view. A NaCl crystal is a typical crystal with various faces of different stability in water. It is known that the preferential adsorption of solvent molecules on particular crystal faces leads to the reduction of their growth rate. Hence the structural and dynamical properties at the water/NaCl interface influence the growth rate of the crystal face and consequently determine the size, the shape, and even other properties of the crystal. Ohtaki et al. investigated the dissolution process of the cubiclike NaCl crystal with (111), $(\bar{1}\bar{1}\bar{1})$, and (001) faces of about 1.2×1.2 nm^2 in water and found that three chloride ions at the corners of the crystal dissolve into water in 7 ps and no sodium ions dissolve from any face.[22] Anastasiou et al. investigated water near the NaCl(001) surfaces and found that water molecules adsorb above sodium ions of the surfaces with their dipoles pointed away from the surfaces and the motion of water molecules near the surfaces is remarkably reduced.[13]

In this study, the characteristics of water molecules near the (001) and (011) faces of NaCl crystals, which are molecularly smooth and stable in vacuum, were investigated in detail and compared, using classical molecular dynamics simulation. First of all, the stability of the (001) or (011) faces of NaCl crystals in water was examined, and then the characteristics of structural and dynamical properties of water molecules near these surfaces were examined. Although both the surfaces are smooth at a molecular level, NaCl(011) is rougher in surface roughness and lower in density of surface ions than NaCl(001). After we confirm that both the NaCl(001) and NaCl(011) surfaces are stable in water at 298 K during the simulation, our attention is mainly focused on how water molecules near the surfaces are influenced by the difference in the nature of surfaces.

In section 2, the details of the molecular models and MD simulations used are described. The Results and Discussion and Conclusions are given in section 3 and section 4, respectively.

2. Methods

A. Molecular Models. Various models for water−water interaction have been proposed. Water models widely used in computer simulations are ST2,[23] MCY,[24] SPC/E(the reparametrized version of the SPC model),[25,26] and TIP4P.[27] The SPC/E model was selected here not only because it more faithfully reproduces the bulk property of water but also because it is more efficient in calculation. The SPC/E water has three point charges, locating $-2q$ on one oxygen atom and $+q$ on two hydrogen atoms ($q = 0.4238e$, e is the elementary charge) and is rigid with 0.1 nm distance between oxygen and hydrogen and 109.74° angle (i.e. a tetrahedral angle) between two OH

* To whom correspondence should be addressed.

S1089-5647(97)02795-8 CCC: $15.00
Published on Web 02/24/1998

TABLE 1: Parameters for Ion−Water Potentials of the Pettitt−Rossky Model

ion (X)	Na^+	Cl^-
$\sigma_{OX}/10^{-10}$ m	2.72	3.55
$\sigma_{HX}/10^{-10}$ m	1.31	2.14
$\epsilon_{OX}/10^{-21}$ J	0.93	2.5
$\epsilon_{HX}/10^{-21}$ J	0.93	2.5

TABLE 2: Parameters for Ion−Ion Potentials of the Tosi−Fumi Model

	Na^+-Na^+	Na^+-Cl^-	Cl^--Cl^-
A_{ij}	1.25	1.00	0.75
$C_{ij}/10^{-79}$ J m^6	1.68	11.2	116.0
$D_{ij}/10^{-99}$ J m^8	0.8	13.9	233.0
$(\sigma_i + \sigma_j)/10^{-10}$ m	2.340	2.755	3.170
$b/10^{-19}$ J	0.338	0.338	0.338
$\rho/10^{-10}$ m	0.317	0.317	0.317

bonds. In addition to the Coulombic potential, there is the Lennard-Jones (12−6) potential between oxygen atoms of a pair of water molecules. The depth of the well ϵ_{OO} and the diameter of the core σ_{OO} are 0.648 kJ/mol and 0.3166 nm, respectively. The hydrogen-bonding energy between two water molecules in their most favorable configuration calculated by this model was reported to be −30.0 kJ/mol.[26]

The Pettitt−Rossky model was used for ion−water interaction.[28] In this model, each ion with one unique charge interacts with three sites of SPC/E water, and the total interaction is given by the summation of the Coulombic and Lennard-Jones (12−6) potentials. The potential parameters used are listed in Table 1.

For the interaction between ions i and j the following Born−Mayer−Huggins potential was used:

$$U_{ij}(r) = \frac{q_i q_j}{r} + A_{ij} b \exp\left(\frac{\sigma_i + \sigma_j - r}{\rho}\right) - \frac{C_{ij}}{r^6} - \frac{D_{ij}}{r^8} \quad (1)$$

where q_i is the ionic charge and A_{ij} the Pauling factor. The values of parameters b, σ_i, ρ, C_{ij}, and D_{ij} given by Tosi and Fumi as in Table 2 were used.[29]

To our knowledge, the potential function between a water molecule and NaCl crystal surfaces based on the ab initio molecular orbital calculation has not been reported. Although the model for ion/water interaction used here was derived for Na^+ and Cl^- ions solvated in water,[28] we evaluated the water/surface interaction by adding this pair potential between a water molecule and ions composing the NaCl crystal layers; that is, the water/surface interaction is treated as "physisorption" in this study. In Figure 1 the potential energy between a water molecule and the NaCl surface with (001) or (011) faces is shown as a function of the distance from the surface for different relative positions and orientations. The interaction energy between a water molecule and the Na^+ adsorption site on NaCl-(001) exhibits a minimum of −43 kJ/mol at the water−surface distance of 0.24 nm, which agrees well with the minimum ranging from −46 to −29 kJ/mol at the distance 0.23 nm obtained from the ab initio periodic Hartree−Fock calculations[32] and the measured value of the differential heat of adsorption of 44 kJ/mol.[30] On the basis of this result we think that the adsorbate/surface interaction is plausibly treated in this study. Comparison of potential curves in parts a and b of Figure 1 indicates that the interaction of the NaCl(011) surface with a water molecule is stronger than that of NaCl(001). It is worth noting that in the case of NaCl(011) the binding energies of a water molecule between two nearest-neighboring Na^+ ions and above a Na^+ ion are equal to −81 and −64 kJ/mol, respectively,

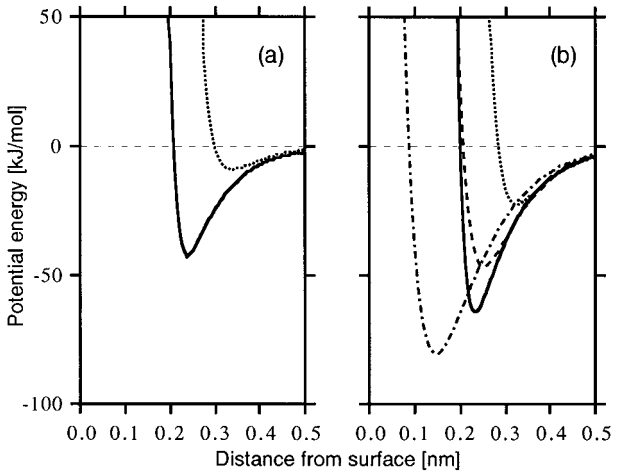

Figure 1. Water/NaCl interaction potential as a function of the distance along the normal to the NaCl surface for different relative positions and orientations: above a Na^+ ion (solid lines) and between two nearest-neighboring Na^+ ions (dashed−dotted line) with the water dipole moment pointing away from the surface, and above a Cl^- ion (dotted lines) and between two nearest-neighboring Cl^- ions (dashed line) with the dipole moment pointing toward the surface. (a) NaCl(001); (b) NaCl(011).

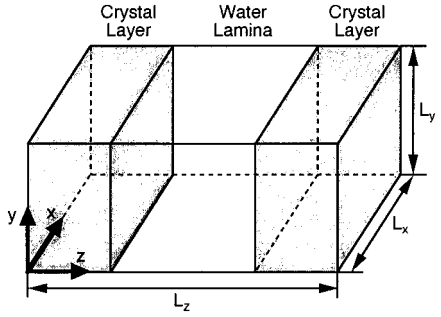

Figure 2. Basic cell for MD simulations. Shaded regions represent the NaCl crystal, and the rest is water. The origin of coordinates is the center of the cell, and the periodic boundary conditions are applied to the three directions.

which are several times larger in absolute value than the hydrogen-bonding energy between two water molecules of −30.0 kJ/mol.[26] Here we emphasize that a slight difference in the surface geometry of crystals causes a significant change in the potential energy between a water molecule and a surface and subsequently leads to a considerable difference in the structural and dynamical properties of water molecules near these surfaces as discussed below.

B. Simulation Details. The simulation was performed using the program based on MDMPOL.[31] The equations of translational and rotational motions were integrated according to the leap-frog method. Figure 2 shows the basic cell used for the present study. The rectangular cell is composed of the central lamina, which contains 216 water molecules, and a NaCl slab with either 12 lattice planes of 6 × 6 ions for the (001) face or 24 lattice planes of 4 × 6 ions for the (011) face. It was confirmed by allowing the ions to move freely at 298 K that these crystal slabs are of stable thickness to keep their structural and dynamical properties solidlike in vacuum. The dimensions of the simulation box are summarized in Table 3, where the origin of coordinates was taken at the center of the water lamina and the xy plane was taken to be parallel to the NaCl surface. The side lengths L_x and L_y were chosen such that the lattice constant of a NaCl crystal is equal to 0.5641 nm. Under these conditions the ions in the first row of NaCl surfaces were located

TABLE 3: Conditions of the Molecular Dynamics Simulations of Water Confined between the NaCl(001) or NaCl(011) Surfaces

		water/NaCl(001)	water/NaCl(011)
side length	L_x/nm	1.692	1.595
	L_y/nm	1.692	1.692
	L_z/nm	5.641	7.180
location of the first-row ions	$\|z\|$/nm	1.26	1.28
cutoff distance	r_c/nm	0.746	0.698
one-time step/fs		1	1
average temperature/K		298	298

at the distance given in Table 3, such that the density of water at the central region is equal to 1 g/cm^3. The periodic boundary conditions were applied to the three directions, and the Ewald summation technique was used to calculate the long-range Coulomb interactions. The non-Coulomb interactions between centers of mass of molecules were cut off at the distance r_c listed in Table 3, without using the site−site cutoff procedure.

The simulation procedure is as follows. After water of density 1 g/cm^3 and crystal slabs were equilibrated separately at 298 K, they were put together. Then the ions in the crystal were fixed and water molecules were allowed to reequilibrate for 15−20 ps. When the stability of the NaCl surfaces in water was examined, the ions were allowed to move further up to 10 ps with the initial velocity corresponding to translational motions at 298 K. The average temperature of the simulations was kept at 298 K by velocity scaling to compensate the change of temperature due to the nonequilibrium processes such as dissolution of ions. The time step used was 1 fs. When the structural and dynamical properties of water near the NaCl surfaces were examined, the ions in the NaCl crystals were fixed and the simulations for water molecules were carried out up to 15 ps without any scaling. The average temperature was found to be 298 K. Although the simulation time of 10−15 ps is on the short side, we believe that the results presented here are reasonable and qualitatively correct.

3. Results and Discussion

A. Stability of NaCl Surfaces. The NaCl surfaces were confirmed to be stable in vacuum as described above, but this does not necessarily guarantee that they are stable in water. Here the stability of NaCl(001) and NaCl(011) surfaces exposed to water was examined. It was found that no ion is dissolved from both NaCl(001) and (011) surfaces into water during 10 ps. The ions in the first row fluctuated around their average positions actively, but the structure of NaCl(001) and NaCl(011) was kept the same as the crystal in the central region. No significant difference in fluctuation was observed between the ions at the interfaces of NaCl(001) and NaCl(011). These results indicate that the NaCl(001) and NaCl(011) faces without any lattice defect are stable in water at 298 K, at least within a short period of our computer simulation, 10 ps, which is in good coincidence with the results predicted by Ohtaki et al.[22] Since no significant change of the structure from that of the bulk crystal was observed, it is plausible to assume that all the ions in the NaCl crystals are fixed at the time-averaged position in the successive simulation.

In the following sections, the structural and dynamical properties of water adjacent to NaCl(001) and NaCl(011) surfaces are discussed in terms of density profiles, numbers of hydrogen bonds and nearest neighbors, trajectories, orientational distributions, and diffusion coefficients, where the parameters given by the function z are averaged with the values at $\pm z$ except for trajectories.

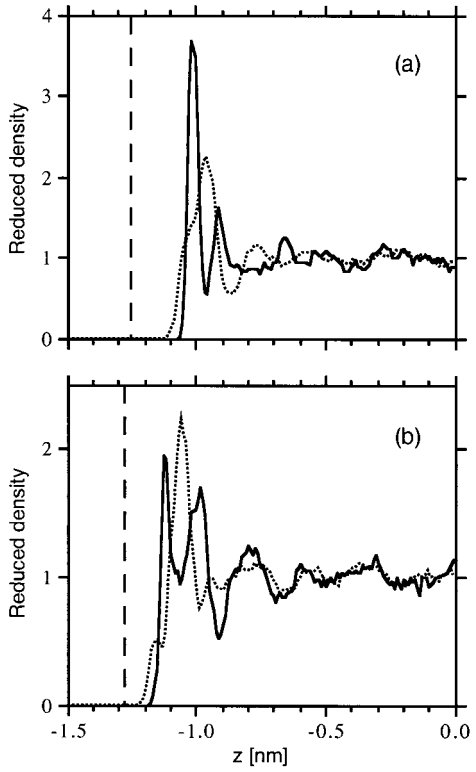

Figure 3. Density profiles of oxygen (solid lines) and hydrogen (dotted lines). The centers of ions in the first row are designated by vertical dashed lines (see Table 4). (a) NaCl(001); (b) NaCl(011).

TABLE 4: Location of the First Three Layers (L1, L2, and L3) and the Middle Layer (LB) Parallel to the *xy* Plane. $N_{water}(i)$ Is the Average Number of Water Molecules in Layer *i*, and $N_{site}(i)$ Is the Number of Typical Adsorption Sites of Water Molecules in Layer *i*

		water/NaCl(001)	water/NaCl(011)
range of $\|z\|$/nm	L1	0.96−1.07	1.07−1.18
	L2	0.81−0.96	0.92−1.07
	L3	0.60−0.81	0.70−0.92
	LB	0.00−0.60	0.00−0.70
$N_{water}(1)/N_{site}(1)$		17.7/18	10.8/12
$N_{water}(2)/N_{site}(2)$		15.3/18	16.0/12

B. Density Profiles of Water. The reduced density profiles of oxygen and hydrogen atoms are shown in Figure 3. Sharp peaks in the oxygen profile are observed in the vicinity of the interface, reflecting that many water molecules are attracted to the surfaces and form an adsorbed layer. It is known that this tendency is characteristic at the interface between water and a hydrophilic plane,[7−11,13−15,17] whereas the hydrophobic surfaces tend to repel water toward the bulk.[6] Comparison between the profiles in Figure 3a,b suggests that the structure of water next to NaCl(001) and NaCl(011) is different from each other. Two sharp peaks in the oxygen profile of NaCl(001) indicate that at least two adsorbed layers of water molecules are formed at the interface, while the three peaks for NaCl(011) indicate that at least three layers are formed. Since the second peak of the oxygen profile in Figure 3b has a shoulder at $|z| = 1.02$ nm near the peak at $|z| = 0.99$ nm, the second layer is considered to be the "bilayer" that is composed of water molecules adsorbed on different relative positions of the surface.

To analyze further the properties of these layers, the water lamina was divided into three regions of the adsorbed layers of water molecules (L1, L2, and L3) and the central region (LB) as listed in Table 4. The minimum distance between the first layer L1 and the center of ions in the first row is 0.19 nm for

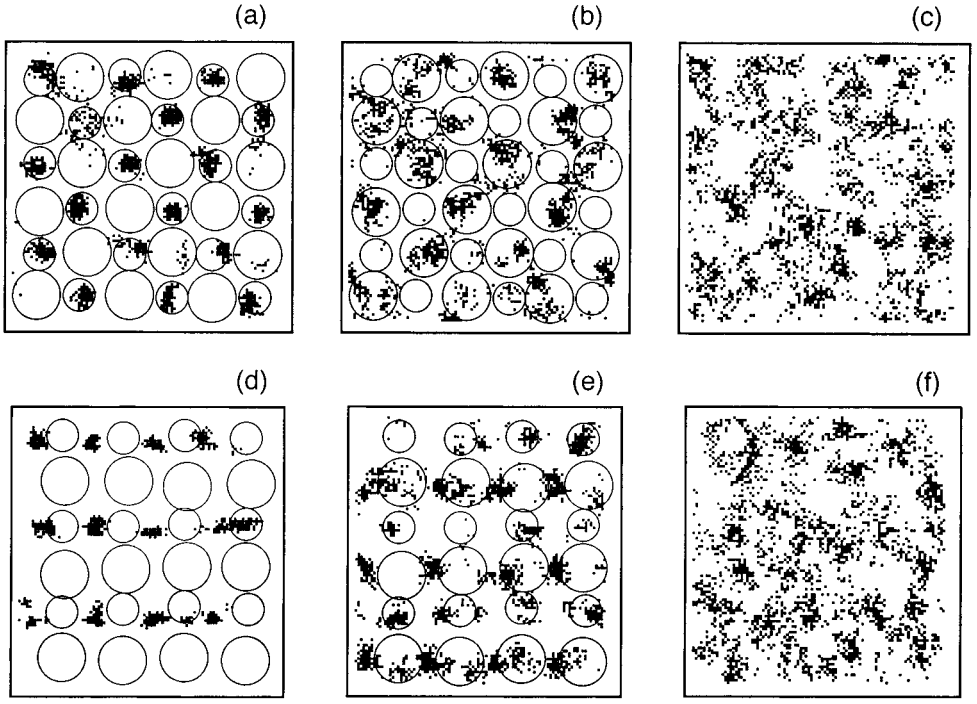

Figure 4. Projected trajectories of oxygen atoms in L1, L2, and L3 (as defined in Table 4) on the NaCl(001) (a, b, and c) and NaCl(011) (d, e, and f) surfaces. Positions of oxygen atoms (x, y) are marked by dots every 0.1 ps for 15 ps. Small circle, sodium ion of the surface; large circle, chloride ion of the surface. In panels c and f, surface ions are omitted because water molecules in L3 have no particular adsorption site.

NaCl(001) and 0.10 nm for NaCl(011), which indicates that water molecules can approach the NaCl(011) surface about 0.1 nm closer than the NaCl(001) surface. This is probably due to the following reasons: (1) the NaCl(011) surface is rougher in geometry than the NaCl(001) surface and (2) a water molecule interacts with the NaCl(011) surface more strongly than the NaCl(001) surface, as shown in Figure 1.

Average numbers of water molecules in L1 and L2 were calculated by integrating the oxygen density profile in each layer as listed in Table 4 with the number of typical adsorption sites for water molecules in each layer (see Figure 4). In the case of NaCl(001), the adsorption sites for L1 were occupied completely, and those for L2 were 80% occupied. On the other hand, the adsorption sites for L1 were 90% covered, but those for L2 were fully covered in the case of NaCl(011). This will explain the presence of the "bilayer" described above.

C. Trajectories of Water Molecules. Projected trajectories of oxygen atoms in the first three layers are illustrated in Figure 4 every 0.1 ps for 15 ps. A glance at Figure 4 suggests that the adsorption sites of water molecules on the NaCl(001) and NaCl(011) surfaces are different. In the case of NaCl(001), water molecules in L1 adsorb above sodium ions and those in L2 adsorb above chloride ions. In the case of NaCl(011), water molecules in L1 adsorb between the two nearest-neighboring sodium ions and those in L2 adsorb mainly between the two nearest-neighboring chloride ions. As shown in Figure 4e, water molecules in L2 adsorb above sodium ions of NaCl(011), corresponding to the presence of a shoulder in the second peak of oxygen profile as mentioned above (see Figure 3b). This result implies that sodium ions at the NaCl(011) surface are masked by hydrated water molecules partly in L2 as well as in L1.

Thus the adsorption sites of water molecules in L1 and L2 are different in the NaCl(001) and NaCl(011) surfaces. In both cases, water molecules in L1 tend to adsorb to the sodium ions somewhat more strongly than those in L2 adsorb to the chloride ions, as expected from Figure 1. However, water molecules in L3 behave apparently more fluidlike because of having no particular adsorption site on the surface, as illustrated in Figure 4c,f.

D. Local Coordination and Hydrogen Bonding. It is known that the network of hydrogen bonding between water molecules is sensitive to the environment around them. A pair of water molecules was regarded as nearest neighbors if their O−O distance is smaller than or equal to 0.35 nm, the distance of the first minimum of the O−O radial distribution function of SPC/E water.[26] They are regarded as hydrogen bonded if they are nearest neighbors and have a pair interaction energy less than or equal to the critical value $\epsilon_{HB} = -10$ kJ/mol simultaneously. Figure 5 shows the average number of nearest neighbors n_{NN} and hydrogen bonds n_{HB} per water molcule as a function of z. It was confirmed that the distributions of n_{HB} are not influenced qualitatively by the threshold values of ϵ_{HB}. It is clear that the values of n_{NN} and n_{HB} at $|z| < 0.5$ nm are almost constant, at about 5.0 and 3.5, respectively, which coincide with those obtained in our calculation of the bulk water. However, the value of n_{HB} is reduced remarkably near the interface, which coincides well with the reduction of the value of n_{NN}. This behavior is similar to that of water near SiO_2,[16] lecithin,[16] and fully hydroxylated silica surfaces.[7] It seems that this behavior is characteristic of water close to the polar or hydrophilic surfaces, although there exists some ambiguity because the value of n_{HB} is reduced only slightly in the case of the Pt(100) surface.[8]

The value n_{HB}/n_{NN}, which is a parameter to evaluate the fraction of hydrogen bonds out of the nearest-neighboring water molecules, was calculated as shown in Figure 6. It exhibits clearly that the hydrogen-bonding network is disrupted remarkably at the NaCl(011) interface, while the network is destroyed at the NaCl(001) interface much less than expected from the significant decrease of n_{HB} shown in Figure 5a. This is because the interaction between a water molecule and the adsorption site of NaCl(011) is much stronger than the hydrogen bond

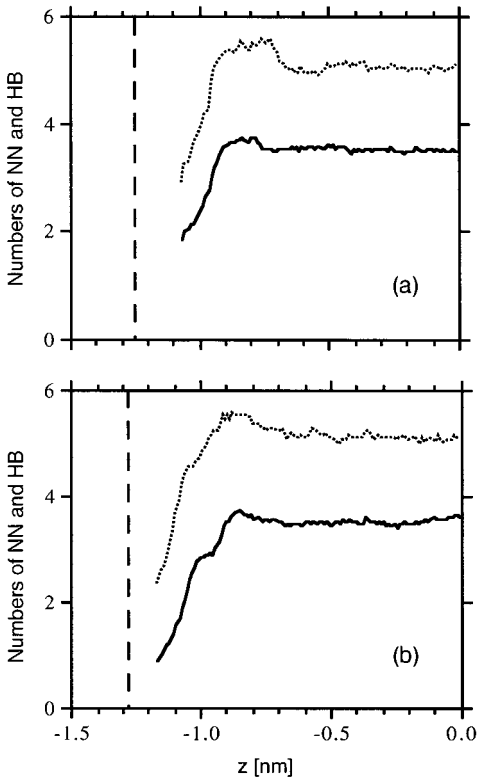

Figure 5. Average numbers of nearest neighbors n_{NN} (dotted lines) and hydrogen bonds n_{HB} (solid lines) per water molecule. The centers of ions in the first row are designated by vertical dashed lines (see Table 4). (a) NaCl(001); (b) NaCl(011).

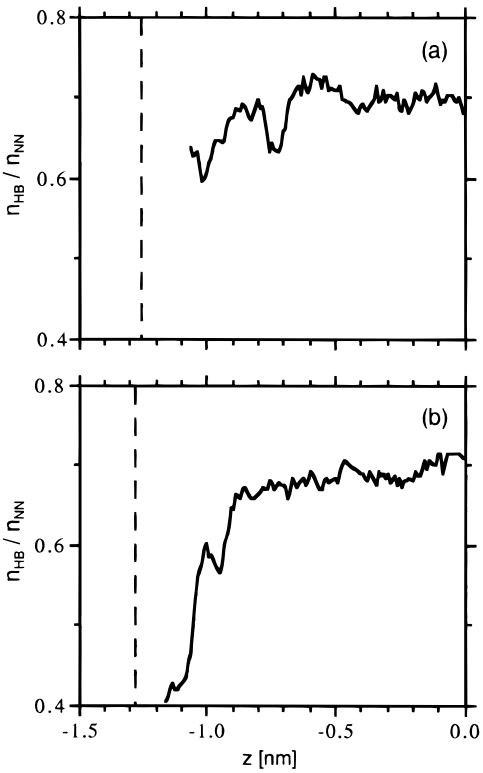

Figure 6. Values of n_{HB}/n_{NN} obtained from Figure 5, which are a parameter to estimate the fraction of hydrogen bonds out of the nearest-neighboring water molecules. The centers of ions in the first row are designated by vertical dashed lines (see Table 4). (a) NaCl(001); (b) NaCl(011).

between two water molecules, while that for NaCl(001) is as strong as the hydrogen bond.

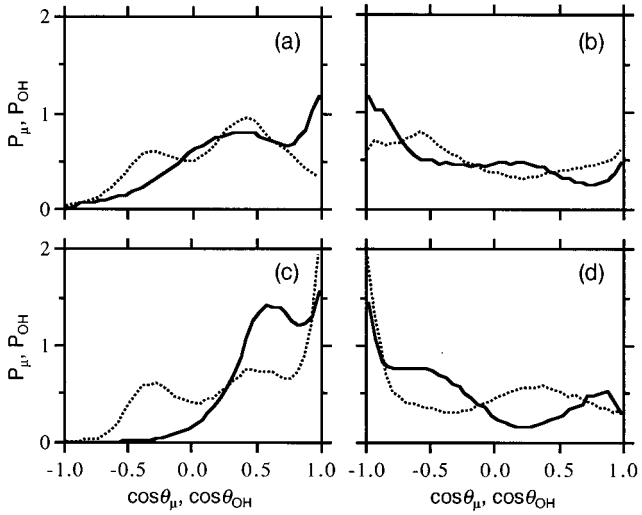

Figure 7. Orientational distributions $P_\mu(\cos\theta_\mu)$ (solid lines) and $P_{OH}(\cos\theta_{OH})$ (dotted lines) for L1 and L2 (as defined in Table 4) on NaCl(001) (a and b) and on NaCl(011) (c and d), where θ_μ is defined as the angle between the dipole vector and the surface normal $\boldsymbol{n}_z$ pointing away from the surface and θ_{OH} as the angle between the vector of the OH bond and $\boldsymbol{n}_z$.

In the case of hydrophobic surfaces, on the other hand, it is known that the value of n_{HB}/n_{NN} increases significantly, although the value of n_{HB} is reduced.[6] This has been explained in such a way that the formation of the "icelike" structure is preferential at the hydrophobic interfaces, while lateral diffusion of water molecules is more fluidlike than that in the bulk.[6,7]

E. Orientational Structures. The results presented above exhibit that the structure of water molecules near the NaCl surface is influenced greatly by the features of the surface. Here the orientational structure of water molecules was investigated in detail. θ_μ was defined as the angle between the dipole vector of a water molecule and the surface normal $\boldsymbol{n}_z$ pointing away from the NaCl surface, θ_{OH} as the angle between the vector of the OH bond and $\boldsymbol{n}_z$, and ϕ_{HH} as the angle between the projection of the HH vector on the *xy* plane and the *x* axis. One- and two-dimensional distributions of these angles for the molecules in L1 and L2 were evaluated. The frequency distributions of $P_\mu(\cos\theta_\mu)$ and $P_{OH}(\cos\theta_{OH})$ are shown in Figure 7, and those of $P_{\mu,HH}(\cos\theta_\mu, \phi_{HH})$ in Figure 8, which were averaged by considering the symmetric features of the NaCl(001) and NaCl(011) surfaces. The distributions in Figures 7 and 8 allow us to determine the favorable configurations of water molecules near the surface, as illustrated in Figure 9, by the procedure described below.

Figure 7 suggests that the orientational structure near the NaCl(001) is different from that near the NaCl(011), as expected from the difference in density profiles and in the adsorption sites of water molecules near the surfaces. The distributions for NaCl(011) have sharper peaks than those for NaCl(001). This is explained by the strong interaction between a water molecule and the NaCl(011) surface, as predicted from the comparison between parts a and b of Figure 1.

In the case of L1 on NaCl(011), the two maxima of P_μ exist at $\cos\theta_\mu = 1.0$ and 0.6, as shown in Figure 7c, which indicates that L1 is made of two types of "flip-up" molecules as illustrated in Figure 9e,f. Here molecules are named "flip-up" and "flop-down" when their dipoles are pointing away from the surface and toward the surface, respectively. The flip-up molecule shown in Figure 9e, whose dipole is parallel to $\boldsymbol{n}_z$ because of $\cos\theta_\mu = 1.0$, has its two OH bonds 55° from $\boldsymbol{n}_z$, because the peak of P_{OH} is observed at $\cos\theta_{OH} = 0.6$. This *z*-oriented water

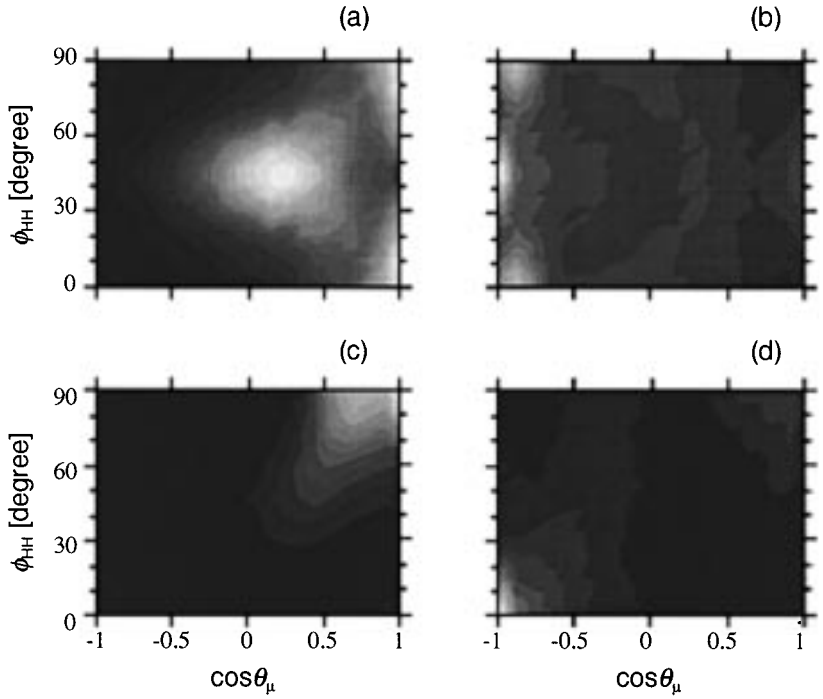

Figure 8. Two-dimensional distributions of orientations $P_{\mu,HH}(\cos\theta_\mu, \phi_{HH})$ for L1 and L2 (as defined in Table 4) on NaCl(001) (a and b) and on NaCl(011) (c and d). θ_μ is defined as the angle between the dipole vector and the surface normal $\boldsymbol{n}_z$ pointing away from the surface, and ϕ_{HH} as the angle between the projection of the HH vector on the *xy* plane and the *x* axis. Distributions were averaged by considering the symmetric geometry of NaCl(001) and NaCl(011) surfaces. The region of the more probable orientation is colored lighter gray. Gray levels in the four panels were used arbitrarily.

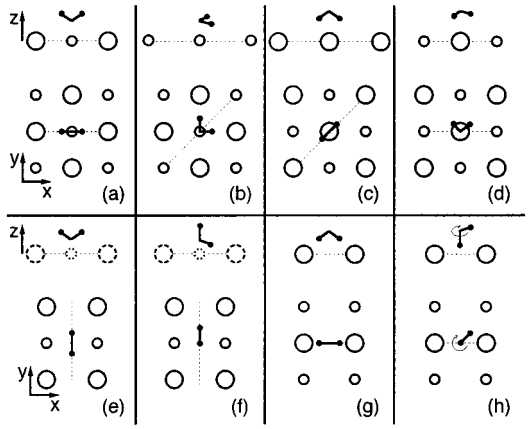

Figure 9. Favorable configurations of a water molecule near the surface for different relative positions. (a, b) L1 on NaCl(001); (c, d) L2 on NaCl(001); (e, f) L1 on NaCl(011); (g, h) L2 on NaCl(011). In each panel, the bottom picture represents the projection of a water molecule on the *xy* plane and the top picture represents its projection on the plane that is perpendicular to the *xy* plane and is crossing through the dashed line drawn in the bottom picture.

molecule tends to be aligned with its HH vector perpendicular to the *x* axis, as shown in Figure 9e, because one of the most probable orientations is given by $(\cos\theta_\mu, \phi_{HH}) = (1.0, 90°)$, as in Figure 8c. For the other flip-up molecule shown in Figure 9f, the two peaks of P_{OH} in Figure 7c located at $\cos\theta_{OH} = 1.0$ and -0.3 indicate that one of its hydrogens is pointing away from the surface (i.e. $\cos\theta_{OH} = 1.0$), while the second hydrogen is creating a tetrahedral angle with the first hydrogen (i.e. $\cos\theta_{OH} = -0.3$), which corresponds to the maximum of P_μ at $\cos\theta_\mu = 0.60$. This *z*-oriented water molecule tends to be aligned with a 90° angle between its projected HH vector on the *xy* plane and the *x* axis, as shown in Figure 9f, because one of the maximal values in $P_{\mu,HH}$ is observed at $(\cos\theta_\mu, \phi_{HH}) = (0.60, 90°)$, as shown in Figure 8c.

When Figure 7c is reversed with respect to $\cos\theta_\mu = 0$ and $\cos\theta_{OH} = 0$, it becomes qualitatively similar to Figure 7d. This indicates that water molecules in L2 favor the two flop-down configurations shown in Figure 9g,h, which are the inverted configurations of Figure 9e,f with respect to the surface plane, respectively. One flop-down molecule with $\cos\theta_\mu = -1.0$ shown in Figure 9g, whose dipole is parallel to $\boldsymbol{n}_z$, orients with its HH vector parallel to the *x* axis because the value of $P_{\mu,HH}$ is maximal at $(\cos\theta_\mu, \phi_{HH}) = (-1.0, 0°)$, as shown in Figure 8d. For the other flop-down molecule with $\cos\theta_\mu = -0.6$, $P_{\mu,HH}$ around $\cos\theta_\mu = -0.6$ does not depend particularly on ϕ_{HH}, suggesting that this water molecule points toward the surface with one OH bond vector, around which the other OH vector can rotate freely, as illustrated in Figure 9h. It is worth noting that P_μ in Figure 7d and $P_{\mu,HH}$ in Figure 8d have their minor peaks around $\cos\theta_\mu = 0.85$, which coincides with the observation that water molecules in L2 near NaCl(011) adsorb above sodium ions, as shown in Figure 4e.

In the case of NaCl(001), on the other hand, one of the maximal values in $P_{\mu,HH}$ is observed at $(\cos\theta_\mu, \phi_{HH}) = (1.0, 0°)$ (and $(1.0, 90°)$) for L1 and $(-1.0, 45°)$, for L2, as shown in parts a and b of Figure 8, respectively, which corresponds to the peaks of P_μ and P_{OH} located at $\cos\theta_\mu = 1.0$ and $\cos\theta_{OH} = 0.6$ for L1 and at $\cos\theta_\mu = -1.0$ and $\cos\theta_{OH} = -0.6$ for L2, respectively. From these results, the favorable configurations for L1 and L2 are depicted in parts a and c of Figure 9, respectively. These complete flip-up and complete flop-down molecules, whose dipoles are parallel to $\boldsymbol{n}_z$, are observed near the NaCl(011) surfaces also, apart from differences in positions of adsorption and in orientations for the projected HH vector on the *xy* plane. The other maximal value in $P_{\mu,HH}$ is located at $(\cos\theta_\mu, \phi_{HH}) = (0.25, 45°)$, for L1, as shown in Figure 8a, and at $(-0.80, 0°)$ (and $(-0.80, 90°)$) for L2, as shown in Figure 8b. For this flip-up molecule in L1, the peaks of P_{OH} are observed at $\cos\theta_{OH} \approx 0.4$ and -0.3, as shown in Figure 7a,

TABLE 5: Diffusion Coefficients of Water Molecules in the Different Layers (in 10^{-5} cm^2/s). L1, L2, L3, and LB Refer to the First Three Layers and to the Middle Layer, Respectively (As Defined in Table 4)

	water/NaCl(001)				water/NaCl(011)			
	L1	L2	L3	LB	L1	L2	L3	LB
D_x	0.13	0.34	1.51	3.06	<0.01	0.66	1.95	3.53
D_y	0.12	0.37	1.73	2.51	0.03	0.30	0.94	2.84
D_z	<0.01	0.04	0.20	1.79	<0.01	0.04	0.24	2.50

which indicates that one of its two hydrogen atoms is pointing away from the surface (i.e. $\cos\theta_{OH} \approx 0.4$), while the other is pointing toward the surface (i.e. $\cos\theta_{OH} \approx -0.3$), as illustrated in Figure 9b. Similarly for this flop-down molecule in L2, although P_{OH} in Figure 7b has no sharp peak, we concluded from the location of the maximal value in $P_{\mu,HH}$ shown in Figure 8b that the two hydrogen atoms are pointing toward the surface, one of which is closer to the surface than the other, as illustrated in Figure 9d. These two z-dependent configurations shown in Figure 9b,d are not dominant near the NaCl(011) surface.

Hydrogen bonding is possible between the water molecules with such configurations as shown in Figure 9a−d, for example between the molecules in parts b and d of Figure 9, but hydrogen bonding between the water molecules in Figure 9e−h is apparently impossible. These results will explain the observation that the hydrogen-bonding network is disrupted near the NaCl(011) surface much more than near the NaCl(001) surface, as shown in Figure 6.

F. Dynamical Properties. The motion of water molecules in the first three layers is illustrated in Figure 4. Here their quantitative motion was investigated in terms of the diffusional coefficients D_α of water molecules in the regions of L1, L2, L3, and LB. The values of D_α in the direction α within each layer were calculated by using the following equation and are shown in Table 5:

$$D_\alpha = \lim_{t\to\infty} \frac{\langle \Delta\alpha^2 \rangle}{2t} \quad (\alpha = x, y, z) \tag{2}$$

It is found that the diffusion coefficients in L1, L2, and L3 are reduced significantly, compared with that for bulk water, 2.5 $\times$ 10^{-5} cm^2/s at 300 K,[26] and are anisotropic because of $D_x \approx D_y > D_z$. The diffusional motion of water molecules decreases as they approach the surface. Especially, water in L1 and L2 on NaCl(001) and NaCl(011) is "solidlike" since this diffusion coefficient is much smaller than that of fluid water. As far as lateral diffusion coefficients D_{xy} (=$(D_x + D_y)/2$) are concerned, water in L1 on the NaCl(011) is more solidlike than that on the NaCl(001), as expected from the difference in their binding energy of a water molecule on the surface. On the other hand, water in L2 on the NaCl(011) is less solidlike than that on the NaCl(001), although the binding energy is larger in absolute value for NaCl(011) than for NaCl(001). This result is explained by the fact that the hydrogen-bonding network near the NaCl(011) surface was disrupted more significantly than that near the NaCl(001), as shown in Figure 6. Thus the binding energy between a water molecule and adsorption sites and the hydrogen-bonding energy must be taken into account simultaneously to explain the diffusional properties of water near the surfaces.

The values of D_x and D_y in the first three layers are isotropic in the case of NaCl(001) as expected from the symmetric geometry C_{4v}, while these coefficients are anisotropic in the case of NaCl(011) because of its surface geometry C_{2v}. At the water/NaCl(011) interface, the x-directed diffusion in L1 is negligibly small because the favorable configuration of adsorbed molecules on NaCl(011) does not allow water molecules to diffuse along the x axis. The value of D_y in L2 is also smaller than that of D_x because the favorable configuration and the "ridge" structure along the x axis of adsorbed water molecules in L1 prohibit the diffusion of water molecules along the y axis, as shown in Figures 9g and 4d. The similar anisotropy of diffusional motion is observed also for molecules in L3. These results indicate that the diffusional motion of water close to the surface is very sensitive to the nature of the surface. It is also found that diffusion coefficients for molecules in LB confined by NaCl(001) or NaCl(011) surfaces are anisotropic. This indicates that water in LB does not display the same dynamical properties as the bulk water, although it has the same static properties as the bulk water, such as density in Figure 3 and the hydrogen-bonding network in Figure 5.

4. Conclusions

Classical molecular dynamics simulations of water/NaCl(001) and water/NaCl(011) interfaces were carried out and the following conclusions were drawn.

(1) The NaCl crystals with both the (001) and (011) faces without any lattice defects are stable in water at 298 K, at least within the period of 10 ps.

(2) Water molecules in L1 and L2 near the NaCl(001) and NaCl(011) surfaces display solidlike properties. However, a slight difference in the features between NaCl(001) and NaCl(011) surfaces causes a significant change in the interactions between a water molecule and the surfaces, the number of adsorbed layers of water, the positions of water molecules, the perturbation of the hydrogen-bonding network, and the detailed diffusional motion near the surface.

(3) Water molecules in LB can be regarded as bulk with respect to their static properties, but the dynamical properties are still influenced by the existence of the crystal surfaces.

Acknowledgment. Computation time of the Cray Y-MP2E/264 and Cray T-94/4128 was provided by the Supercomputer Laboratory, Institute for Chemical Research, Kyoto University.

References and Notes

(1) Matsumoto, M.; Kataoka, Y. *J. Chem. Phys.* **1988**, *88*, 3233.
(2) Townsend, R. M.; Rice, S. A. *J. Chem. Phys.* **1991**, *94*, 2207.
(3) Carpenter, I. L.; Hehre, W. J. *J. Phys. Chem.* **1990**, *94*, 531.
(4) Benjamin, I. *J. Chem. Phys.* **1992**, *97*, 1432.
(5) Smit, B.; Hilbers, P. A. J.; Esselink, K.; Rupert, L. A. M.; van Os, N. M.; Schlijper, A. G. *J. Phys. Chem.* **1991**, *95*, 6361.
(6) Lee, C. Y.; McCammon, J. A.; Rossky, P. J. *J. Chem. Phys.* **1984**, *80*, 4448.
(7) Lee, S. H.; Rossky, P. J. *J. Chem. Phys.* **1994**, *100*, 3334.
(8) Spohr, E. *J. Phys. Chem.* **1989**, *93*, 6171.
(9) Spohr, E. *Chem. Phys.* **1990**, *141*, 87.
(10) Raghavan, K.; Foster, K.; Motakabbir, K.; Berkowitz, M. *J. Chem. Phys.* **1991**, *94*, 2110.
(11) Raghavan, K.; Foster, K.; Berkowitz, M. *Chem. Phys. Lett.* **1991**, *177*, 426.
(12) Siepmann, J. I.; Sprik, M. *J. Chem. Phys.* **1995**, *102*, 511.
(13) Anastasiou, N.; Fincham, D.; Singer, K. *J. Chem. Soc., Faraday Trans. 2* **1983**, *79*, 1639.
(14) McCarthy, M. I.; Schenter, G. K.; Scamehorn, C. A.; Nicholas, J. B. *J. Phys. Chem.* **1996**, *100*, 16989.
(15) Kjellander, R.; Marčelja, S. *Chem. Scr.* **1985**, *25*, 73.
(16) Kjellander, R.; Marčelja, S. *Chem. Phys. Lett.* **1985**, *120*, 393.
(17) Boek, E. S.; Briels, W. J.; van Eerden, J.; Feil, D. *J. Chem. Phys.* **1992**, *96*, 7010.
(18) Marrink, S.-J.; Berendsen, H. J. C. *J. Phys. Chem.* **1994**, *98*, 4155.
(19) Heller, H.; Schaefer, M.; Schulten, K. *J. Phys. Chem.* **1993**, *97*, 8343.
(20) Shinoda, W.; Namiki, N.; Okazaki, S. *J. Chem. Phys.* **1997**, *106*, 5731.
(21) Toney, M. F.; Howard, J. N.; Richer, J.; Borges, G. L.; Gordon, J. G.; Melroy, O. R.; Wiesler, D. G.; Yee, D.; Sorensen, L. B. *Nature* **1994**, *368*, 444.

(22) Ohtaki, H.; Fukushima, N. *Pure Appl. Chem.* **1989**, *61*, 179.
(23) Stillinger, F. H.; Rahman, A. *J. Chem. Phys.* **1974**, *60*, 1545.
(24) Matsuoka, O.; Clementi, E.; Yoshimine, M. *J. Chem. Phys.* **1976**, *64*, 1351.
(25) Berendsen, H. J. C.; Postma, J. P. M.; van Gunsteren, W. F.; Hermans, J. In *Intermolecular Forces: Proceedings of the Fourteenth Jerusalem Symposium on Quantum Chemistry and Biochemistry*; Pullman, B., Ed.; Reidel: Dordrecht, 1981; p 331.
(26) Berendsen, H. J. C.; Grigera, J. R.; Straatsma, T. P. *J. Phys. Chem.* **1987**, *91*, 6269.
(27) Jorgensen, W. L.; Chandrasekhar, J.; Madura, J. D.; Impey, R. W.; Klein, M. L. *J. Chem. Phys.* **1983**, *79*, 926.
(28) Pettitt, B. M.; Rossky, P. J. *J. Chem. Phys.* **1986**, *84*, 5836.
(29) Fumi, F. G.; Tosi, M. P. *J. Phys. Chem. Solids* **1964**, *25*, 31. Tosi, M. P.; Fumi, F. G. *J. Phys. Chem. Solids* **1964**, *25*, 45.
(30) Barraclough, P. B.; Hall, P. G. *Surf. Sci.* **1974**, *46*, 393.
(31) Smith, W.; Fincham, D. *CCP5 Newsletter*; Daresbury Laboratory: Warrington, England, 1982.
(32) Taylor, D. P.; Hess, W. P.; McCarthy, M. I. *J. Phys. Chem. B* **1997**, *101*, 7455.